How well does nonrelativistic QCD factorization work for inclusive quarkonium production at NLO?

Xiang-Peng Wang (TUM)

Nora Brambilla & Mathias Butenschön

arXiv: 2411.16384

HF-HNC 2024,

China Hotel, Guangzhou

06 -11 Dec. 2024

Outlines

1. Review of inclusive quarkonium production in NRQCD

2. Our fit-and-prediction descriptions in NRQCD at NLO

3. Summary

Quarkonium: A multi-scale problem

- Quarkonium: Excellent probe of PDFs, GPDs, TMDs, QGP.... Referred as the QCD version of hydrogen atom – The simplest QCD system.
- Quarkonium production at colliders is a typical multi-scale problem
  - m_Q, the heavy-quark mass scale, $m_c \sim 1.5$ GeV, $m_b \sim 4.75$ GeV;
  - $m_Q v$, the typical heavy-quark momentum;
  - $m_Q v^2$, the typical heavy-quark kinetic energy and binding energy.
- v is the typical heavy-quark velocity in the quarkonium rest frame,
  - $v^2 \simeq 0.25$ for charmonium;
  - $v^2 \simeq 0.1$ for bottomonium.
- 50 year passed since the discovery of J/ψ, its production mechanism is not fully understood yet. Puzzles still remain.

Nonrelativistic QCD (NRQCD) factorization

- Nonrelativistic QCD (NRQCD) factorization is the most prominent approach to describe both quarkonium decay and production processes.
  Bodwin, Braaten & Lepage, PRD 51, 1125 (1995), ~ 3000 citations.

$$\sigma_{\mathcal{Q}+X} = \sum_n \hat{\sigma}\left(ij \to Q\bar{Q}(n) + X\right) \langle \mathcal{O}^{\mathcal{Q}}(n)\rangle, \tag{1}$$

  with $i, j = \{p, \bar{p}, e^+, e^-, \gamma, \gamma^*, ...\}$, $n = {}^{2S+1}L_J^{[1/8]}$, $[1], [8]$ representing color-singlet (CS) and color-octet (CO), respectively.

- $\hat{\sigma}$, the short-distance-coefficients (SDCs), $Q\bar{Q}$ in state n produced at short distance, α_s expansion,

- $\langle \mathcal{O}^{\mathcal{Q}}(n)\rangle$, long-distance-matrix-elements (LDMEs), supposed to be universal, describing the hadronization $Q\bar{Q}(n) \to \mathcal{Q} + X$, v^2 expansion.

- NRQCD factorization: double expansion of α_s, v^2.

p_T power counting

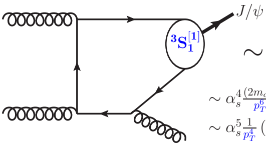

$\sim \alpha_s^3 \frac{(2m_c)^4}{p_T^8}$

$\sim \alpha_s^4 \frac{(2m_c)^2}{p_T^6}$ (NLO)

$\sim \alpha_s^5 \frac{1}{p_T^4}$ (NNLO)

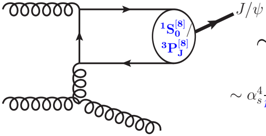

$\sim \alpha_s^3 \frac{(2m_c)^2}{p_T^6} v^4$

$\sim \alpha_s^4 \frac{1}{p_T^4} v^4$ (NLO)

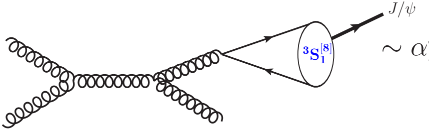

$\sim \alpha_s^3 \frac{1}{p_T^4} v^4$

- At high p_T, p_T power counting dominates (over α_s, v^2 power counting).
- At LO, only ${}^3S_1^{[8]}$ channel gives p_T leading-power (LP, $1/p_T^4$) contribution, which leads to strong transverse polarization (The J/ψ polarization puzzle!).
- We need NLO calculation to include other LP contributions (CS contribution is small even at NNLO). Lansberg, EPJC 61, 693 (2009)

Heavy quark spin symmetry (HQSS)

- For the spin-1 S-wave quarkonium V $(J/\psi, \Upsilon ...)$, based on HQSS, we have

$$\langle \mathcal{O}^V({}^3P_J^{[8]})\rangle = (2J+1)\langle \mathcal{O}^V({}^3P_0^{[8]})\rangle(1+\mathcal{O}(v^2)). \quad (2)$$

- Relations between the LDMEs of η_c and J/ψ due to HQSS,

$$\langle \mathcal{O}^{\eta_c}({}^1S_0^{[1]}/{}^1S_0^{[8]})\rangle = \frac{1}{3}\langle \mathcal{O}^{J/\psi}({}^3S_1^{[1]}/{}^3S_1^{[8]})\rangle(1+\mathcal{O}(v^2)), \quad (3)$$

$$\langle \mathcal{O}^{\eta_c}({}^3S_1^{[8]})\rangle = \langle \mathcal{O}^{J/\psi}({}^1S_0^{[8]})\rangle(1+\mathcal{O}(v^2)), \quad (4)$$

$$\langle \mathcal{O}^{\eta_c}({}^1P_1^{[8]})\rangle = 3\langle \mathcal{O}^{J/\psi}({}^3P_0^{[8]})\rangle(1+\mathcal{O}(v^2)). \quad (5)$$

NRQCD long-distance-matrix elements (LDMEs)

The definitions of the relevant spin-1 S-wave quarkonium (V) LDMEs are

$$\langle \mathcal{O}^V({}^3S_1^{[1]})\rangle = \langle\Omega|\chi^\dagger\sigma^i\psi\mathcal{P}_{V(\boldsymbol{P}=\mathbf{0})}\psi^\dagger\sigma^i\chi|\Omega\rangle, \tag{6a}$$

$$\langle \mathcal{O}^V({}^3S_1^{[8]})\rangle = \langle\Omega|\chi^\dagger\sigma^i T^a\psi\Phi_\ell^{\dagger ab}\mathcal{P}_{V(\boldsymbol{P}=\mathbf{0})}\Phi_\ell^{bc}\psi^\dagger\sigma^i T^c\chi|\Omega\rangle, \tag{6b}$$

$$\langle \mathcal{O}^V({}^1S_0^{[8]})\rangle = \langle\Omega|\chi^\dagger T^a\psi\Phi_\ell^{\dagger ab}\mathcal{P}_{V(\boldsymbol{P}=\mathbf{0})}\Phi_\ell^{bc}\psi^\dagger T^c\chi|\Omega\rangle, \tag{6c}$$

$$\langle \mathcal{O}^V({}^3P_0^{[8]})\rangle = \frac{1}{3}\langle\Omega|\chi^\dagger(-\tfrac{i}{2}\overleftrightarrow{\boldsymbol{D}}\cdot\boldsymbol{\sigma})T^a\psi\Phi_\ell^{\dagger ab}\mathcal{P}_{V(\boldsymbol{P}=\mathbf{0})} \times \Phi_\ell^{bc}\psi^\dagger(-\tfrac{i}{2}\overleftrightarrow{\boldsymbol{D}}\cdot\boldsymbol{\sigma})T^c\chi|\Omega\rangle, \tag{6d}$$

here $\mathcal{P}_{V(\boldsymbol{P})} = \sum_X |V+X\rangle\langle V+X|$, $\Phi_\ell = P\exp[-ig\int_0^\infty d\lambda\,\ell\cdot A^{\mathrm{adj}}(\ell\lambda)]$ is the path-ordered Wilson line that ensures the gauge invariance.

- CS LDMEs can be related to quarkonium nonrelativistic wavefunctions.
- Unclear how to calculate CO LDMEs from first principle such as lattice, so the CO LDMEs are determined through fitting with experimental data.

Recent significant progress: Spin-1 S-wave LDMEs in pNRQCD

- Based on strong coupled pNRQCD, we have (up to $\mathcal{O}(1/N_c^2, v^2)$ corrections),
  Brambilla, Chung, Vairo & Wang, PRD105, L111503 (2022); JHEP 03 (2023) 242

$$\langle \mathcal{O}^V(^3S_1^{[1]}) \rangle = 2N_c \times \frac{3|R_V^{(0)}(0)|^2}{4\pi}, \tag{7a}$$

$$\langle \mathcal{O}^V(^3S_1^{[8]}) \rangle = \frac{1}{2N_c m^2} \frac{3|R_V^{(0)}(0)|^2}{4\pi} \mathcal{E}_{10;10}, \tag{7b}$$

$$\langle \mathcal{O}^V(^1S_0^{[8]}) \rangle = \frac{1}{6N_c m^2} \frac{3|R_V^{(0)}(0)|^2}{4\pi} c_F^2 \mathcal{B}_{00}, \tag{7c}$$

$$\langle \mathcal{O}^V(^3P_0^{[8]}) \rangle = \frac{1}{18N_c} \frac{3|R_V^{(0)}(0)|^2}{4\pi} \mathcal{E}_{00}, \tag{7d}$$

- c_F is the NRQCD(HQET) matching coefficient,
- $R_V^{(0)}(0)$ is the wave-function at the origin,
- $\mathcal{E}_{10;10}$, $\mathcal{B}_{00}$, and $\mathcal{E}_{00}$ are universal gluonic correlators of mass dimension 2,

Gluonic correlators

$$\mathcal{E}_{10;10} = \left| d^{dac} \int_0^\infty dt_1\, t_1 \int_{t_1}^\infty dt_2\, gE^{b,i}(t_2) \right.$$
$$\left. \times\, \Phi_0^{bc}(t_1;t_2) gE^{a,i}(t_1) \Phi_0^{df}(0;t_1) \Phi_\ell^{ef} |\Omega\rangle \right|^2, \quad \text{(8a)}$$
$$\mathcal{B}_{00} = \left| \int_0^\infty dt\, gB^{a,i}(t) \Phi_0^{ac}(0;t) \Phi_\ell^{bc} |\Omega\rangle \right|^2, \quad \text{(8b)}$$
$$\mathcal{E}_{00} = \left| \int_0^\infty dt\, gE^{a,i}(t) \Phi_0^{ac}(0;t) \Phi_\ell^{bc} |\Omega\rangle \right|^2, \quad \text{(8c)}$$

where $\Phi_0(t,t') = \mathcal{P} \exp[-ig \int_t^{t'} d\tau\, A_0^{\text{adj}}(\tau, \mathbf{0})]$ is a Schwinger line.

- By evolving the scale of $\mathcal{E}_{10;10}$, $\mathcal{B}_{00}$, and $\mathcal{E}_{00}$ from charm mass scale to bottom mass scale, we can related LDMEs between $\psi(nS)$ and $\Upsilon(nS)$.

pNRQCD predictive power

- Significantly reduces the number of independent CO LDMEs ($15 \to 3$).
- J/ψ and $\psi(2S)$ share the same $\mathcal{E}_{10;10}$, $\mathcal{B}_{00}$, and $\mathcal{E}_{00}$, thus their cross sections ratio equals the ratio of $|R^{(0)}_{J/\psi}(0)|^2$ and $|R^{(0)}_{\psi(2S)}(0)|^2$ (same for $\Upsilon(nS)$ states).

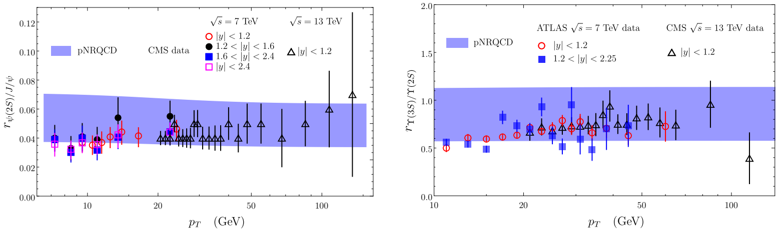

Figures from Brambilla, Chung, Vairo & Wang, JHEP 03 (2023) 242

- The prediction is based on NRQCD factorization and pNRQCD relations of the LDMEs without explicit perturbative calculations!

J/ψ LDMEs fittings

- Chao et al. : $p_T > 7$Gev, two linear combinations (of the 3 CO LDMEs) are constrained, but the best fit gives large $\langle \mathcal{O}^{J/\psi}({}^1S_0^{[8]})\rangle$.

  Ma, Wang & Chao, PRL 106, 042002 (2011)

- Butenschön et al. : $p_T > 3$Gev, global fit (pp, $p\bar{p}$, γp, $\gamma\gamma$, e^+e^-) .

  Butenschön & Kniehl, PRD 84, 051501 (2011)

- Zhang et al. : $p_T > 7$Gev, combine J/ψ and η_c hadron production data based on HQSS, constrains $\langle \mathcal{O}^{J/\psi}({}^1S_0^{[8]})\rangle$ to be small.

  Zhang *et al.*, PRL 114, 092006 (2015)

- Bodwin et al. : $p_T > 10$Gev, combine leading-power resummation with NLO fixed-order calculation.

  Bodwin *et al.*, PRD 93, 034041 (2016)

- Feng et al. : $p_T > 7$Gev, fit both J/ψ hadron production and polarization data.

  Feng *et al.*, PRD 99, 014044 (2019)

- TUM : $p_T > 3(5) \times 2m_Q$, fit 3 gluonic correlators to the high p_T J/ψ, $\psi(2S)$, $\Upsilon(2S/3S)$ hadroproduction data based on the pNRQCD relations, also leads to small $\langle \mathcal{O}^{J/\psi}({}^1S_0^{[8]})\rangle$.

  Brambilla, Chung, Vairo & Wang, PRD105, L111503 (2022); JHEP 03 (2023) 242

J/ψ LDMEs fittings

Table: Selected representative fitting results in units of 10^{-2} GeV^3.

Group	$\langle \mathcal{O}^{J/\psi}(^3S_1^{[8]}) \rangle$	$\langle \mathcal{O}^{J/\psi}(^1S_0^{[8]}) \rangle$	$\langle \mathcal{O}^{J/\psi}(^3P_0^{[8]}) \rangle / m^2$
Chao et al. set 1	0.05	7.4	0
Chao et al. set 2	1.11	0	1.89
Butenschön et al.	0.168 $\pm$ 0.046	3.04 $\pm$ 0.35	$-$ 0.404 $\pm$ 0.072
Zhang et al.	1.0 $\pm$ 0.3	0.74 $\pm$ 0.3	1.7 $\pm$ 0.5
Bodwin et al.	$-$ 0.713 $\pm$ 0.364	11 $\pm$ 1.4	$-$ 0.312 $\pm$ 0.151
Feng et al.	0.117 $\pm$ 0.058	5.66 $\pm$ 0.47	0.054 $\pm$ 0.005
TUM $(p_T > 3 \times 2m_Q)$	1.72$\pm$ 0.18	-4.7$\pm$ 1.55	3.14 $\pm$ 0.35
TUM $(p_T > 5 \times 2m_Q)$	1.57$\pm$ 0.45	-2.73$\pm$ 3.64	2.89$\pm$0.87

- Dramatically different LDME sets are fitted, but none of them can well describe all the data, challenging the LDME universality.
- Fittings are based on NLO calculations, which are rather complicated and need super computer. Inclusive productions at NNLO are infeasible in near future.

Score card of fittings

Table: Tests of the LDMEs for J/ψ from high p_T pp, and low p_T γp, $\gamma\gamma$ collisions. ✓ ✗ indicates marginally well (no serious conflict).

Group	pp (p_T in fit)	pol. (pp)	$\eta_c(pp)$	$J/\psi + Z$	γp	$\gamma\gamma$
Chao et al. set 1	✓ ($p_T > 7$GeV)	✓	✗	-	✗	-
Chao et al. set 2	✓ ($p_T > 7$GeV)	✓	✓	-	✗	-
Butenschön et al.	✓ ($p_T > 3$GeV)	✗	✗	✗	✓	✗
Zhang et al. $+\eta_c$	✓ ($p_T > 6.5$GeV)	✓	✓	-	✗	-
Bodwin et al.	✓ ($p_T > 10$GeV)	✓	✗	✗	✗	-
Feng et al.	✓ ($p_T > 7$GeV)	✓	✗	-	✗	-
TUM (pNRQCD)	✓ ($p_T > 3 \times 2m_Q$)	✓	✗	✓✗	✗	-
TUM (pNRQCD)	✓ ($p_T > 5 \times 2m_Q$)	✓	✓	✓✗	✗	-

The main conflicts/puzzles

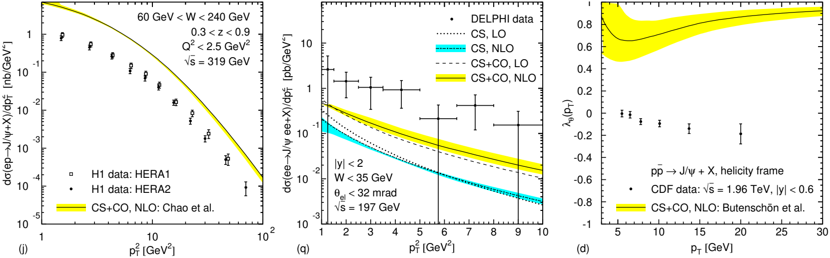

Figures from M. Butenschön, B. A. Kniehl, Mod.Phys.Lett. A 28 (2013) 1350027.

- All high $p_T > 7$GeV fittings overshoot the low p_T γp data by a factor of $\sim 5-10$ (see left figure, take Chao et. al as an example).
- Global fit cannot describe the low p_T $\gamma\gamma$ data and the J/ψ polarization data (see middle and right figures).

Motivations

- The conflict between low p_T and high p_T fittings and descriptions still remain.
- It has been argued that NRQCD factorization may only hold at $p_T \gg 2m_Q$ (see, for instance, the talk of Bodwin at LepageFest 2024). Really?
- Key observation 1: There is no theory prediction for J/ψ p_T distribution in the region $1 \gg z$, although the data exist long time ago (surprising!).
- Key observation 2: There is no theory prediction using high p_T fit for the low p_T LEP data (surprising!), while the global low p_T fit cannot describe the data.
- Another motivation: Describe recent ATLAS (2309.17177, global fit cannot well describe the data at very high p_T) J/ψ production data with p_T ranging from 8 GeV to 360 GeV.

Our new fitting strategies and fitting results

- We combine LHC η_c and J/ψ data to fit 3 J/ψ CO LDMEs based on HQSS.
- We choose three different scale choices, $\mu_r = \mu_f = [\frac{1}{2}, 1, 2]m_T$, with the default scale choice $\mu_r = \mu_f = m_T$, where $m_T = \sqrt{4m_Q^2 + p_T^2}$;
- By choosing: $m_c = 1.5$ GeV, $\langle\mathcal{O}^{J/\psi}({}^3S_1^{[1]})\rangle = 1.16$ GeV^3, $\langle\mathcal{O}^{\psi(2S)}({}^3S_1^{[1]})\rangle = 0.76$ GeV^3 and $\langle\mathcal{O}^{\eta_c}({}^1S_0^{[1]})\rangle = 0.328$ GeV^3,

  we obtain three sets of fitted CO LDMEs with uncertainties, corresponding to the three different scale choices (in units of 10^{-2} GeV^3),

$\mu_r = \mu_f$	$\langle\mathcal{O}^{J/\psi}({}^3S_1^{[8]})\rangle$	$\langle\mathcal{O}^{J/\psi}({}^1S_0^{[8]})\rangle$	$\frac{\langle\mathcal{O}^{J/\psi}({}^3P_0^{[8]})\rangle}{m_c^2}$	$\frac{\chi^2_{\text{min}}}{\text{d.o.f}}$
$m_T/2$	0.604 ± 0.106	-0.501 ± 0.171	0.716 ± 0.169	0.26
m_T	1.062 ± 0.195	-0.204 ± 0.229	1.905 ± 0.422	0.18
$2m_T$	1.367 ± 0.261	0.094 ± 0.288	3.232 ± 0.732	0.15

Fitting results – LHCb η_c production

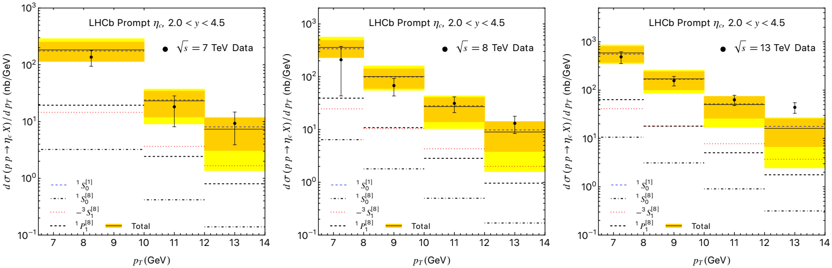

- Inner bands correspond to the default scale choice, the outer bands encompass the uncertainties coming from the two other scale choices.
- The above figures show that CS channel saturates the cross sections and thus can constrain $\langle \mathcal{O}^{J/\psi}({}^1S_0^{[8]}) \rangle$ to be small under HQSS.

Fitting results – CMS J/ψ production

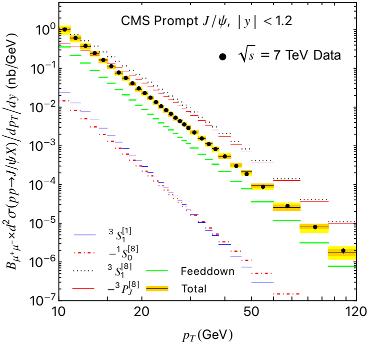

- The cross sections are based on the cancellation between a large positive $^3S_1^{[8]}$ and a large negative $^3P_J^{[8]}$ J/ψ production channel.
- This cancellation is not fine-tuning, because NLO LDME mixing implies that only the sum of both contributions has physical significance.

Prediction – J/ψ polarization

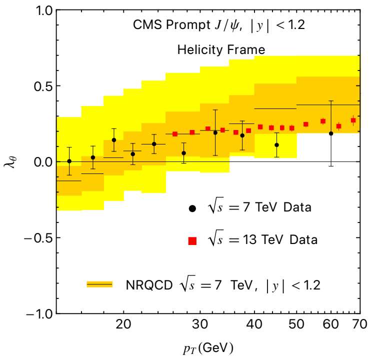

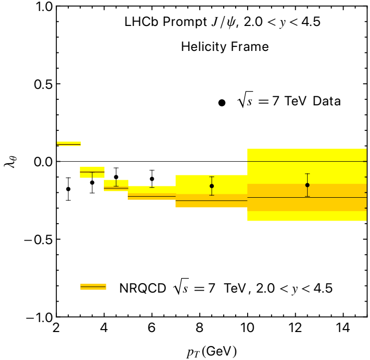

- Our predictions are In good agreement with the measurements and match the pattern that λ_θ turns from slightly negative at relatively low p_T to positive and converges to $\lambda_\theta \sim 0.3$ at high p_T.
- No polarization puzzle appear.

Prediction – ATLAS J/ψ production at very high p_T

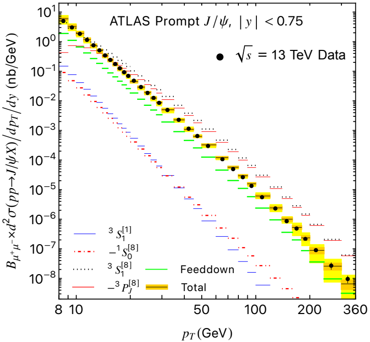

- Excellent description up to the highest measured p_T, supprising!
- Contradicts with the negative cross section predictions (arXiv: 2408.04255).
- It is, however, unclear why it works at very high p_T. The resummation effect of $\log(m_c^2/p_T^2)$ is expected to be significant at very high p_T. Further investigations are needed to understand the deep reasons.

Prediction – LHCb J/ψ production at low p_T

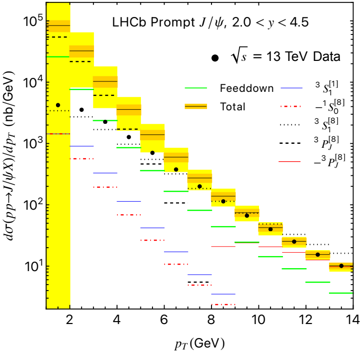

- The $^3P_J^{[8]}$ SDCs change sign from negative to positive when going below $p_T \approx 7$ GeV, so that instead of a cancellation between $^3S_1^{[8]}$ and $^3P_J^{[8]}$ channels, there is an amplification.
- The resulting steep increase at low p_T is not observed in the data.
- Small-x resummation needed.

Prediction – ATLAS $\Upsilon(nS)$ production in pNRQCD

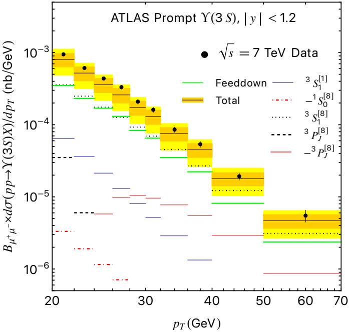

$$\langle \mathcal{O}^V(^3S_1^{[1]})\rangle = 2N_c \times \frac{3|R_V^{(0)}(0)|^2}{4\pi},$$

$$\langle \mathcal{O}^V(^3S_1^{[8]})\rangle = \frac{1}{2N_c m^2}\frac{3|R_V^{(0)}(0)|^2}{4\pi}\mathcal{E}_{10;10},$$

$$\langle \mathcal{O}^V(^1S_0^{[8]})\rangle = \frac{1}{6N_c m^2}\frac{3|R_V^{(0)}(0)|^2}{4\pi}c_F^2\mathcal{B}_{00},$$

$$\langle \mathcal{O}^V(^3P_0^{[8]})\rangle = \frac{1}{18N_c}\frac{3|R_V^{(0)}(0)|^2}{4\pi}\mathcal{E}_{00},$$

$$\mathcal{B}_{00}(m_b) = \mathcal{B}_{00}(m_c)\left(1-\frac{2N_c}{\beta_0}\ln\frac{\alpha_s(m_c)}{\alpha_s(m_b)}\right) \simeq 0.74\times\mathcal{B}_{00}(m_c),$$

$$\mathcal{E}_{10;10}(m_b) = \mathcal{E}_{10;10}(m_c) + \frac{4}{3\beta_0}\frac{N_c^2-4}{N_c}\mathcal{E}_{00}\ln\frac{\alpha_s(m_c)}{\alpha_s(m_b)} \simeq \mathcal{E}_{10;10}(m_c) + 0.1\,\mathcal{E}_{00}.$$

- ATLAS $\Upsilon(3S)$ data well reproduced, similar results for $\Upsilon(1S)$ and $\Upsilon(2S)$.
- Highly nontrivial test of the above pNRQCD relations.
- The scale evolutions of the gluonic correlators (mainly from $\mathcal{E}_{10;10}$, $^3S_1^{[8]}$ LDMEs) result in a very different Fock state decomposition in $\Upsilon(3S)$, where the cross section is dominated by the $^3S_1^{[8]}$ channel and feeddown from χ_{bJ}.

Prediction – ATLAS $J/\psi + Z$, single parton scattering (SPS)

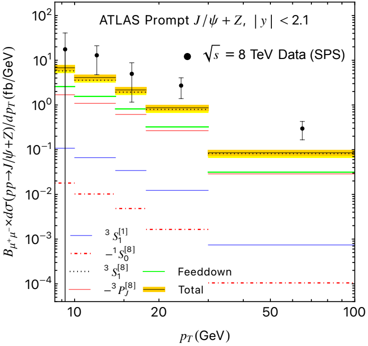

- $^3S_1^{[8]}$ channel dominates. DPS contribution is smaller at higher p_T.
- For the two highest p_T bins, predictions lie $\sim 2\sigma$ deviations below data. Underestimated DPS contributions, unlikely? or?

Prediction – LEP $\gamma\gamma \to J/\psi + X$

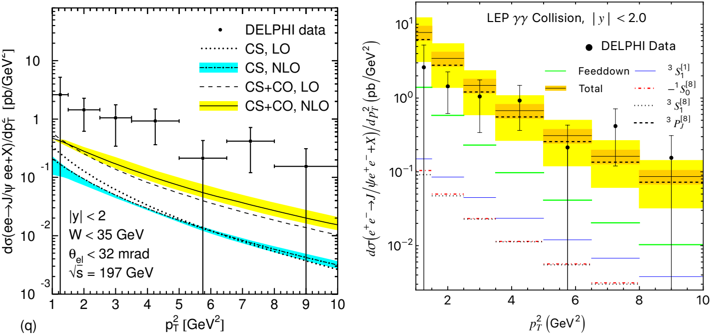

Figure: Left: global fit (Butenschön et al.); right: our prediction

- The cross section is exclusively dominated by single-resolved photon contributions. CS contribution is far below the data. ${}^3P_J^{[8]}$ channels dominate.

Prediction – HERA $\gamma p \to J/\psi + X$ $(0.1 < z < 0.3)$

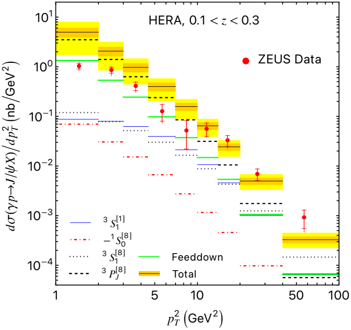

Figure: Our prediction with divided z bins (and figures in the next 2 slides). Inelasticity $z = E_{J/\psi}/E_\gamma$ in the proton rest frame.

- For $0.1 < z < 0.3$, good description for the data except for a few lowest p_T bins, where resolved photon ($gg \to J/\psi + X$) contribution dominates, which is similar to hadroproduction case, so, not surprised.

Prediction – HERA $\gamma p \to J/\psi + X$ $(0.3 < z < 0.6)$

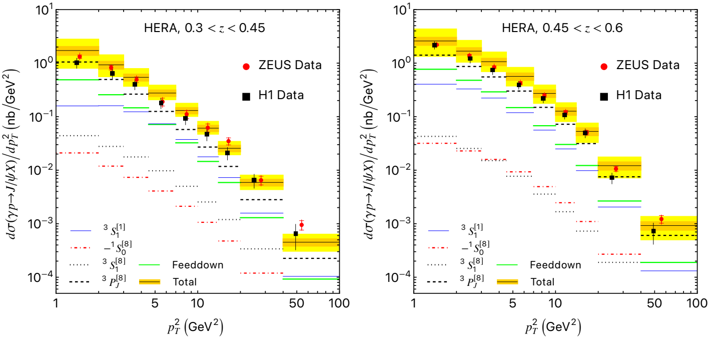

- The data can be well described in the whole measured p_T range, $[1, 10]$GeV.
- ${}^3P_J^{[8]}$ channels dominate, comparing to the ${}^3S_1^{[8]}$, ${}^3P_J^{[8]}$ cancellation scenario in large p_T hadroproduction.

Prediction – HERA $\gamma p \to J/\psi + X$ $(0.6 < z < 0.9)$

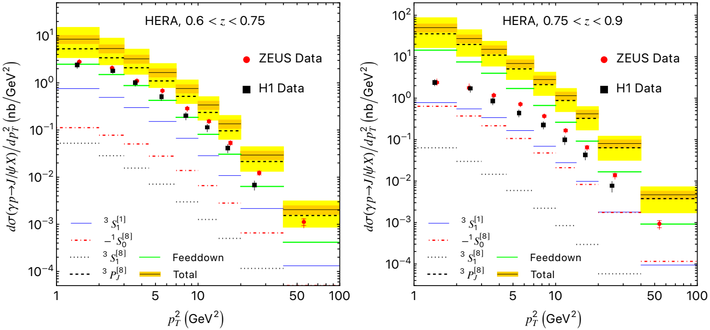

- Obviously overshoot the data, regardless of p_T. For $0.75 < z < 0.9$, predictions overshoot the data by factors of 5.2 to 20.
- The region $z \to 1$ corresponds to the endpoint region, where the NRQCD factorization may not be valid, v^2 expansion becomes $v^2/(1-z)$ expansion. Quarkonium shape function needed. Beneke, Rothstein & Wise, PLB 408, 373 (1997).

Update score card of fittings

Table: Tests of the LDMEs for J/ψ from high p_T pp, and low p_T γp, $\gamma\gamma$ collisions. ✓ ✗ indicates marginally well (no serious conflict).

Group	pp (p_T in fit)	pol. (pp)	η_c (pp)	$J/\psi + Z$	γp	$\gamma\gamma$
Chao et al. set 1	✓ ($p_T > 7$GeV)	✓	✗	-	✗	-
Chao et al. set 2	✓ ($p_T > 7$GeV)	✓	✓	-	✗	-
Butenschön et al.	✓ ($p_T > 3$GeV)	✗	✗	✗	✓	✗
Zhang et al. $+\eta_c$	✓ ($p_T > 6.5$GeV)	✓	✓	-	✗	-
Bodwin et al.	✓ ($p_T > 10$GeV)	✓	✗	✗	✗	-
Feng et al.	✓ ($p_T > 7$GeV)	✓	✗	-	✗	-
TUM (pNRQCD)	✓ ($p_T > 3 \times 2m_Q$)	✓	✗	✓✗	✗	-
TUM (pNRQCD)	✓ ($p_T > 5 \times 2m_Q$)	✓	✓	✓✗	✗	-
This work	✓ ($p_T > 6.5$GeV)	✓	✓	✓✗	✓ ($z < 0.6$)	✓

- Now, J/ψ high p_T hadroproduciton and low $p_T$production from $\gamma p(z < 0.6)$, $\gamma\gamma$ collisions can be consistently described.

Summary

- Simple answer: NRQCD works pretty well except for end-point regions.
- The following data are well reproduced in NRQCD factorization at NLO:
  - High p_T $J/\psi, \eta_c, \Upsilon(nS)$ production ✓ (highly nontrivial test of pNRQCD)
  - High p_T J/ψ polarization ✓ no polarization puzzle!
  - Very high p_T $(360$ GeV$)$ J/ψ production ✓ surprising! (why so well?)
  - J/ψ from $\gamma\gamma$ with $10\,\text{GeV}^2 > p_T^2 > 1\,\text{GeV}^2$ ✓ surprising!
  - J/ψ from γp with $100\,\text{GeV}^2 > p_T^2 > 1\,\text{GeV}^2$, $z < 0.6$ ✓ surprising!
  - $J/\psi + Z$ ✓ ✗ (underestimated DPS contributions, unlikely? or?)
- Challenges the argument that NRQCD factorization may only hold at $p_T \gg 2m_Q$, NRQCD works well at low p_T from $\gamma p, \gamma\gamma$ collisions.
- Observables still evade a consistent description: coincide with “extensions” of endpoint regions.
  - Low p_T hadroproduction ✗ small-x resummation
  - J/ψ photoproduction $(z > 0.6)$, J/ψ from Belle ✗ shape function
- Has significance impact on future quarkonium studies at EIC, EicC, HL-LHC.